The competitive nature of STAT complex formation drives phenotype switching of T cells

STAT signaling in T cell plasticity

Ildar I Sadreev[1,2,*], Michael Z Q Chen[3], Yoshinori Umezawa[4], Vadim N Biktashev[1], Claudia Kemper[5,6,7], Diana V Salakhieva[8], Gavin I Welsh[9], Nikolay V Kotov[10].

[1] Centre for Systems, Dynamics and Control, College of Engineering, Mathematics and Physical Sciences, University of Exeter, Harrison Building, North Park Road, Exeter EX4 4QF, UK
[2] (current address) Section of Experimental Haematology, Leeds Institute of Cancer and Pathology, University of Leeds, Leeds, UK
[3] School of Automation, Nanjing University of Science and Technology, Nanjing 210094, Jiangsu, P. R. China
[4] Department of Dermatology, The Jikei University School of Medicine, 3-25-8 Nishishimbashi, Minato-ku, Tokyo, 105-8461, Japan
[5] Laboratory of Molecular Immunology and Immunology Center, National Heart, Lung and Blood Institute, Bethesda, MD, USA;
[6] Division of Transplant Immunology and Mucosal Biology, King's College London, London, UK
[7] Institute for Systemic Inflammation Research, University of Lübeck, Lübeck, Germany
[8] Institute of Fundamental Medicine and Biology, Kazan (Volga Region) Federal University, 18 Kremlyovskaya St., 420008 Kazan, Russia
[9] Bristol Renal, School of Clinical Sciences, University of Bristol, Dorothy Hodgkin Building, Whitson Street, Bristol, BS1 3NY, UK
[10] Biophysics & Bionics Lab, Institute of Physics, Kazan (Volga Region) Federal University, Kazan 420008, Russia

[*] Corresponding author. Ildar I Sadreev. Section of Experimental Haematology, Leeds Institute of Cancer and Pathology, University of Leeds, Leeds, UK. E-mail: ildar.sadreev@gmail.com

Email addresses:
IIS: ildar.sadreev@gmail.com
MZQC: mzqchen@gmail.com
YU: yoshinori.umezawa@jikei.ac.jp
VNB: v.n.biktashev@exeter.ac.uk
CK: claudia.kemper@nih.gov
DVS: divitsai@gmail.com
GIW: g.i.welsh@bristol.ac.uk
NVK: nvkotov@gmail.com

Key words

Signal transducers and activators of transcription (STATs), T cells, IFN-γ, IL-10, phenotype switching

List of abbreviations

STAT – signal transducer and activator of transcription

IFN-γ – interferon gamma

IL-10 – interleukin 10

Th1 – T helper type 1 cells

Tr1 – type 1 Treg cells

JAK – janus kinase

RA – rheumatoid arthritis

SLE – systemic lupus erythematosus

IBD – inflammatory bowel disease

Summary

Signal transducers and activators of transcription (STATs) are key molecular determinants of T cell fate and effector function. Several inflammatory diseases are characterized by an altered balance of T cell phenotypes and cytokine secretion. STATs, therefore, represent viable therapeutic targets in numerous pathologies. However, the underlying mechanisms by which the same STAT proteins regulate both the development of different T cell phenotypes and their plasticity during changes in extracellular conditions remain unclear. In this study, we investigated the STAT-mediated regulation of T cell phenotype formation and plasticity using mathematical modeling and experimental data for intracellular STAT signaling proteins. The close fit of our model predictions to the experimental data allows us to propose a potential mechanism for T cell switching. According to this mechanism, T cell phenotype switching is due to the relative redistribution of STAT dimer complexes caused by the extracellular

cytokine-dependent STAT competition effects. The developed model predicts that the balance between the intracellular STAT species defines the amount of the produced cytokines and thereby T cell phenotypes. The model predictions are consistent with the experimentally observed IFN-γ to IL-10 switching that regulates human Th1/Tr1 responses. The proposed model is applicable to a number of STAT signaling circuits.

Introduction

Signal transducers and activators of transcription (STATs) regulate cell differentiation, growth, apoptosis and proliferation by transducing signals from the cell membrane to the nucleus. There are seven members of the STAT family in mammalian cells: STAT1, STAT2, STAT3, STAT4, STAT5a, STAT5b and STAT6 (1, 2).

STAT proteins are activated by binding of a cytokine to its receptor followed by receptor dimerization and phosphorylation of their C-terminal transactivation domain (CTD) by janus kinases (JAKs). For example, phosphorylation of STAT1 occurs at Tyr701 in response to type II interferons (3) and phosphorylation of STAT3 occurs at Tyr705 in response to interleukin 6 (IL-6) or interleukin 10 (IL-10) (4, 5). Phosphorylation at Tyr705 leads to dimerization (6) and regulates the activation of STAT3 (7-9). STATs can form homo- or hetero- dimers only with their dimerization partners (10). STAT dimers translocate to the nucleus, activate gene expression and induce cytokine production. Nuclear phosphatases can dephosphorylate STATs in the nucleus and initiate their return to the cytosol (11-14).

Alterations in the mechanism of JAK-STAT activation and cytokine production can give rise to various immune-related pathologies including autoimmune diseases such as rheumatoid arthritis (RA) (15, 16), systemic lupus erythematosus (SLE) (17-19), diabetes (20, 21) and

cancer (22, 23). It was reported in (24) that RA patients lack the so called IFN-γ to IL-10 switching – the transition of the inflammatory IFN-γ only state (Th1 cells) into a state characterized by a significant decrease of IFN-γ production and a gain of the regulatory IL-10 expression (Tr1 cells).

Despite extensive experimental research and recent progress in the treatment of the immune-related pathologies, the cause of such diseases is still not clear due to a lack of understanding of the molecular mechanisms at a systems level. Therefore, in order to further our understanding of the autoimmune states, new systems approaches and mathematical modeling are needed to delineate the molecular mechanisms of T cell phenotype development and plasticity (24, 25). Most of the previous mathematical models (26-28) studied only one signaling pathway at a time, but this limits the power of these models to predict the cellular behavior in response to the interplay of STAT signaling pathways. Indeed in our previous paper (29), we also studied phosphorylation of one STAT protein at a time. In this study, we developed a novel systems model to investigate the role of the interplay between multiple STAT proteins in T cell phenotype plasticity and in IFN-γ to IL-10 switching (24). The developed model integrates separate JAK-STAT signaling pathways into a unified cellular response. The model is based on previously published experimental results (30-46) and supported by the new data.

Materials and Methods

Mathematical model

In this section, a mathematical description of our model for the STAT3-STAT5 subsystem shown in Fig 1B is provided. We investigated the steady state solutions of the phosphorylated proteins (STATs) and produced cytokines. The full information about all the reactions and equations governing STAT3-STAT5, STAT3-STAT4 and the combined

STAT3-STAT4-STAT5 subsystems can be found in Supplementary Materials (Section 2, "Mathematical model").

Cytokine-receptor interactions

Concentrations of phosphorylated Receptor-JAK complexes activated by IL-2, IL-6 and IL-21, respectively, as functions of the corresponding cytokine concentration can be written as follows:

$$
\begin{aligned}
[w2] &= -\frac{M_2 - r2_t + p2_t\left(\frac{M_1}{n_1[i2]} + \frac{1}{n_1} + 1\right)}{2} + \\
&+ \frac{\sqrt{\left(M_2 - r2_t + p2_t\left(\frac{M_1}{n_1[i2]} + \frac{1}{n_1} + 1\right)\right)^2 + 4r2_t M_2}}{2}, \\
[w6] &= -\frac{M_4 - r6_t + p6_t\left(\frac{M_3}{n_2[i6]} + \frac{1}{n_2} + 1\right)}{2} + \\
&+ \frac{\sqrt{\left(M_4 - r6_t + p6_t\left(\frac{M_3}{n_2[i6]} + \frac{1}{n_2} + 1\right)\right)^2 + 4r6_t M_4}}{2}, \\
[w21] &= -\frac{M_6 - r21_t + p21_t\left(\frac{M_5}{n_3[i21]} + \frac{1}{n_3} + 1\right)}{2} + \\
&+ \frac{\sqrt{\left(M_6 - r21_t + p21_t\left(\frac{M_5}{n_3[i21]} + \frac{1}{n_3} + 1\right)\right)^2 + 4r21_t M_6}}{2},
\end{aligned}
\tag{1}
$$

where $[i2] = \frac{[IL\text{-}2]}{STAT3_T}$, $[w2] = \frac{[IL2Rp{:}JAK]}{STAT3_T}$, $r2_t = \frac{IL2R_T}{STAT3_T}$, $p2_t = \frac{SHP\text{-}1_T}{STAT3_T}$, $[i6] = \frac{[IL\text{-}6]}{STAT3_T}$, $[w6] = \frac{[IL6Rp{:}JAK]}{STAT3_T}$, $r6_t = \frac{IL6R_T}{STAT3_T}$, $p6_t = \frac{SHP\text{-}2_T}{STAT3_T}$, $[i21] = \frac{[IL\text{-}21]}{STAT3_T}$, $[w21] = \frac{[IL21Rp{:}JAK]}{STAT3_T}$, $r21_t = \frac{IL21R_T}{STAT3_T}$, $p21_t = \frac{P21_T}{STAT3_T}$ (here subscripts *t* and *T* denote the

total amount of protein in non-dimensional and dimensional forms, respectively, small p stands for the phosphorylated state), M_1, M_2, M_3, M_4, M_5 and M_6 are the non-dimensional Michaelis constants, n_1, n_2 and n_3 denote the ratio of receptor phosphorylation/dephosphorylation rates. Equations (1) follow from the stationary conditions of the phosphorylation and dephosphorylation of the receptors mentioned previously. The derivation of Equations (1) can be found in Supplementary Materials, Equations (S2)-(S13).

STAT phosphorylation and dimerization

STAT proteins are phosphorylated by the activated interleukin-receptor-JAK complexes $\mathrm{IL2Rp{:}JAK}$, $\mathrm{IL6Rp{:}JAK}$ and $\mathrm{IL21Rp{:}JAK}$ (Fig 1B). The biochemical reactions involved in STAT activation are given by:

$$\begin{aligned}
&\mathrm{IL2Rp{:}JAK} + \mathrm{STAT3} \underset{a_3}{\overset{a_1}{\rightleftarrows}} \mathrm{IL2Rp{:}JAK{:}STAT3} \xrightarrow{a_2} \mathrm{IL2Rp{:}JAK} + \mathrm{STAT3p} \\
&\mathrm{IL6Rp{:}JAK} + \mathrm{STAT3} \underset{a_6}{\overset{a_4}{\rightleftarrows}} \mathrm{IL6Rp{:}JAK{:}STAT3} \xrightarrow{a_5} \mathrm{IL6Rp{:}JAK} + \mathrm{STAT3p} \\
&\mathrm{SHP\text{-}1} + \mathrm{STAT3p} \underset{a_9}{\overset{a_7}{\rightleftarrows}} \mathrm{SHP\text{-}1 : STAT3p} \xrightarrow{a_8} \mathrm{SHP\text{-}1} + \mathrm{STAT3} \\
&\mathrm{IL2Rp{:}JAK} + \mathrm{STAT5} \underset{a_{12}}{\overset{a_{10}}{\rightleftarrows}} \mathrm{IL2Rp{:}JAK{:}STAT5} \xrightarrow{a_{11}} \mathrm{IL2Rp{:}JAK} + \mathrm{STAT5p} \\
&\mathrm{IL21Rp{:}JAK} + \mathrm{STAT5} \underset{a_{15}}{\overset{a_{13}}{\rightleftarrows}} \mathrm{IL21Rp{:}JAK{:}STAT5} \xrightarrow{a_{14}} \mathrm{IL21Rp{:}JAK} + \mathrm{STAT5p} \qquad (2) \\
&\mathrm{SHP\text{-}2} + \mathrm{STAT5p} \underset{a_{18}}{\overset{a_{16}}{\rightleftarrows}} \mathrm{SHP\text{-}2{:}STAT5p} \xrightarrow{a_{17}} \mathrm{SHP\text{-}2} + \mathrm{STAT5} \\
&\mathrm{STAT3p} + \mathrm{STAT3p} \underset{a_{20}}{\overset{a_{19}}{\rightleftarrows}} \mathrm{STAT3{:}STAT3} \\
&\mathrm{STAT3p} + \mathrm{STAT5p} \underset{a_{22}}{\overset{a_{21}}{\rightleftarrows}} \mathrm{STAT3{:}STAT5} \\
&\mathrm{STAT5p} + \mathrm{STAT5p} \underset{a_{24}}{\overset{a_{23}}{\rightleftarrows}} \mathrm{STAT5{:}STAT5}
\end{aligned}$$

The corresponding ordinary differential equations (ODEs) for Reactions (2) can be written as follows:

$$\frac{d}{dt}[IL2Rp{:}JAK{:}STAT3] = a_1[IL2Rp{:}JAK][STAT3] - (a_2 + a_3)[IL2Rp{:}JAK{:}STAT3],$$

$$\frac{d}{dt}[IL6Rp{:}JAK{:}STAT3] = a_4[IL6Rp{:}JAK][STAT3] - (a_5 + a_6)[IL6Rp{:}JAK{:}STAT3],$$

$$\begin{aligned}\frac{d}{dt}[STAT3p] = {} & a_2[IL2Rp{:}JAK{:}STAT3] + a_5[IL6Rp{:}JAK{:}STAT3] - \\ & -a_7[SHP\text{-}1][STAT3p] + a_9[SHP\text{-}1{:}STAT3p] - 2a_{19}[STAT3p]^2 + \\ & +2a_{20}[STAT3{:}STAT3] - a_{21}[STAT3p][STAT5p] + a_{22}[STAT3{:}STAT5],\end{aligned}$$

$$\frac{d}{dt}[SHP\text{-}1{:}STAT3p] = a_7[SHP\text{-}1][STAT3p] - (a_8 + a_9)[SHP\text{-}1{:}STAT3p],$$

$$\frac{d}{dt}[IL2Rp{:}JAK{:}STAT5] = a_{10}[IL2Rp{:}JAK][STAT5] - (a_{11} + a_{12})[IL2Rp{:}JAK{:}STAT5],$$

$$\frac{d}{dt}[IL21Rp{:}JAK{:}STAT5] = a_{13}[IL21Rp{:}JAK][STAT5] - (a_{14} + a_{15})[IL21Rp{:}JAK{:}STAT5], \qquad (3)$$

$$\begin{aligned}\frac{d}{dt}[STAT5p] = {} & a_{11}[IL2Rp{:}JAK{:}STAT5] + a_{14}[IL21Rp{:}JAK{:}STAT5] - \\ & -a_{16}[SHP\text{-}2][STAT5p] + a_{18}[SHP\text{-}2{:}STAT5p] - a_{21}[STAT3p][STAT5p] + \\ & +a_{22}[STAT3{:}STAT5] - 2a_{23}[STAT5p]^2 + 2a_{24}[STAT5{:}STAT5],\end{aligned}$$

$$\frac{d}{dt}[SHP\text{-}2{:}STAT5p] = a_{16}[SHP\text{-}2][STAT5p] - (a_{17} + a_{18})[SHP\text{-}2{:}STAT5p],$$

$$\frac{d}{dt}[STAT3{:}STAT3] = a_{19}[STAT3p]^2 - a_{20}[STAT3{:}STAT3],$$

$$\frac{d}{dt}[STAT3{:}STAT5] = a_{21}[STAT3p][STAT5p] - a_{22}[STAT3{:}STAT5],$$

$$\frac{d}{dt}[STAT5{:}STAT5] = a_{23}[STAT5p]^2 - a_{24}[STAT5{:}STAT5].$$

Conservation equations of the total proteins concentrations are given by:

$$\begin{aligned}STAT3_T = {} & [STAT3] + [STAT3p] + 2[STAT3{:}STAT3] + [STAT3{:}STAT5] + \\ & + [IL2Rp{:}JAK{:}STAT3] + [IL6Rp{:}JAK{:}STAT3] + [SHP\text{-}1{:}STAT3p], \\ STAT5_T = {} & [STAT5] + [STAT5p] + 2[STAT5{:}STAT5] + [STAT3{:}STAT5] + \\ & + [IL2Rp{:}JAK{:}STAT5] + [IL21Rp{:}JAK{:}STAT5] + [SHP\text{-}2{:}STAT5p], \\ SHP\text{-}1_T = {} & [SHP\text{-}1] + [SHP\text{-}1{:}STAT3p], \\ SHP\text{-}2_T = {} & [SHP\text{-}2] + [SHP\text{-}2{:}STAT5p].\end{aligned} \qquad (4)$$

Conservation Equations (4) can be written in a non-dimensional form:

$$
\begin{aligned}
1 &= [s3] + [s3p] + 2[s33] + [s35] + [w2s3] + [w6s3] + [p3s3p], \\
s5_t &= [s5] + [s5p] + 2[s55] + [s35] + [w2s5] + [w21s5] + [p5s5p], \\
p3_t &= [p3] + [p3s3p], \\
p5_t &= [p5] + [p5s5p], \\
pp_t &= [pp] + [pps3p],
\end{aligned} \tag{5}
$$

where we introduced the non-dimensional concentrations of the proteins normalized by

$$
STAT3_T : [s3] = \frac{[STAT3]}{STAT3_T},\ [s3p] = \frac{[STAT3p]}{STAT3_T},\ [w2s3] = \frac{[IL2Rp{:}JAK{:}STAT3]}{STAT3_T},
$$

$$
[w6s3] = \frac{[IL6Rp{:}JAK{:}STAT3]}{STAT3_T},\ [p3s3p] = \frac{[SHP\text{-}1{:}STAT3p]}{STAT3_T},\ s5_t = \frac{STAT5_T}{STAT3_T},\ [s5] = \frac{[STAT5]}{STAT3_T},
$$

$$
[s5p] = \frac{[STAT5p]}{STAT3_T},\ [w2s5] = \frac{[IL2Rp{:}JAK{:}STAT5]}{STAT3_T},\ [w21s5] = \frac{[IL21Rp{:}JAK{:}STAT5]}{STAT3_T},
$$

$$
[p5s5p] = \frac{[SHP\text{-}2{:}STAT5p]}{STAT3_T},\ [s33] = \frac{[STAT3{:}STAT3]}{STAT3_T},\ [s35] = \frac{[STAT3{:}STAT5]}{STAT3_T},
$$

$$
[s55] = \frac{[STAT5{:}STAT5]}{STAT3_T},\ [p3] = \frac{[SHP\text{-}1]}{STAT3_T},\ [p5] = \frac{[SHP\text{-}2]}{STAT3_T},\ p3_t = \frac{SHP\text{-}1_T}{STAT3_T},\ p5_t = \frac{SHP\text{-}2_T}{STAT3_T}.
$$

In order to find the steady-state solutions of Equations (3) we need to solve the following system of algebraic equations:

$$
\begin{cases}
0 = [s3p] + 2\dfrac{[s3p]^2}{M_{13}} + \dfrac{[s3p][s5p]}{M_{14}} + \dfrac{p3_t[s3p]}{M_9 + [s3p]}\left(1 + \dfrac{M_7 + [w2] + M_7Q_6}{n_4[w2] + n_5M_7Q_6}\right) - 1, \\
0 = [s5p] + 2\dfrac{[s5p]^2}{M_{15}} + \dfrac{[s3p][s5p]}{M_{14}} + \dfrac{p5_t[s5p]}{M_{12} + [s5p]}\left(1 + \dfrac{M_{10} + [w2] + M_{10}Q_{21}}{n_6[w2] + n_7M_{10}Q_{21}}\right) - s5_t,
\end{cases} \tag{6}
$$

where $M_7 = \dfrac{a_2 + a_3}{a_1 STAT3_T}$, $M_8 = \dfrac{a_5 + a_6}{a_4 STAT3_T}$, $M_9 = \dfrac{a_8 + a_9}{a_7 STAT3_T}$, $M_{10} = \dfrac{a_{11} + a_{12}}{a_{10} STAT3_T}$,

$M_{11} = \dfrac{a_{14} + a_{15}}{a_{13} STAT3_T}$, $M_{12} = \dfrac{a_{17} + a_{18}}{a_{16} STAT3_T}$, $M_{13} = \dfrac{a_{20}}{a_{19} STAT3_T}$, $M_{14} = \dfrac{a_{22}}{a_{21} STAT3_T}$,

$M_{15} = \dfrac{a_{24}}{a_{23} STAT3_T}$ are the non-dimensional Michaelis constants, $Q_6 = \dfrac{[w6]}{M_8}$ and $Q_{21} = \dfrac{[w21]}{M_{11}}$.

System (6) was solved numerically to obtain steady-state concentrations of STAT proteins as a function of IL-2.

SP1 activation

There is an additional, STAT-independent, mechanism for the regulation of IL-10 production. Pathogens can activate the c3-c3b complement system, which leads to the activation of CD46 (46). CD46 can facilitate the production of IL-10 through the SPAK-ERK pathway and SP1 transcription factor in the presence of high concentrations of IL-2 (24). This dependence is described by hypothetical enzymatic reactions shown in supplementary Equations (S33). Thus, it can be written for the concentration of the active SP1 in non-dimensional form:

$$[sp1a] = sp1_t \frac{[i2]}{M_{16} + [i2]} \frac{[cd46]}{M_{17} + [cd46]}, \tag{7}$$

where $[sp1a] = \frac{[SP1a]}{STAT3_T}$, $sp1_t = \frac{SP1_T}{STAT3_T}$, $[cd46] = \frac{[CD46]}{STAT3_T}$, M_{16} and M_{17} are the Michaelis constants.

Cytokine production

The production of IFN-γ and IL-10 is induced by STAT dimer interactions with the genes responsible for production of IFN-γ and IL-10 (33). The produced cytokine can be degraded by a factor of degradation Mp (cytokine-receptor binding, diffusion and cleavage by metalloproteases) (47). The concentration of the produced IFN-γ in non-dimensional form can be written as follows:

$$[ig] = \frac{M_{18}}{\frac{mp1_t}{n_8 gg_t \frac{[s55]}{M_{19} + [s55]}} - 1}, \tag{8}$$

where $[ig] = \frac{[IFN\text{-}\gamma]}{STAT3_T}$, $mp1_t = \frac{Mp1_T}{STAT3_T}$, $gg_t = \frac{Gene_T^{IFN\text{-}\gamma}}{STAT3_T}$, M_{18} and M_{19} are the Michaelis constants, n_8 is the ratio of IFN-γ production to degradation rates. In order to achieve the

steady-state, IFN-γ production rate should be less than its maximal degradation rate, which implies $n_8 < 1$.

Both STAT3:STAT3 homodimer and CD46 (through SPAK-ERK pathway) can activate the same IL-10 gene but they bind different binding regions, as shown in (48). IL-10 is produced after the binding of either of the transcription factors to the gene, which corresponds to (49). Thus it can be written for IL-10 concentration:

$$[i10] = \frac{M_{20}}{\frac{mp2_t}{n_9 g10_t\left(\frac{[s33]}{M_{21}+[s33]} + \frac{[sp1a]}{M_{22}+[sp1a]} - \frac{[s33]}{M_{21}+[s33]}\frac{[sp1a]}{M_{22}+[sp1a]}\right)} - 1}, \quad (9)$$

where $[i10] = \frac{[IL\text{-}10]}{STAT3_T}$, $mp2_t = \frac{Mp2_T}{STAT3_T}$, $g10_t = \frac{Gene_T^{IL\text{-}10}}{STAT3_T}$, $n_9 = \frac{l_6}{k_{11}}$, M_{20}, M_{21} and M_{22} are the Michaelis constants, n_9 is the ratio of IL-10 production to degradation rates, $n_9 < 1$. Equations (8) and (9) are used to describe the concentration of produced IFN-γ and IL-10 as a function of IL-2.

Equations (7), (8) and (9) are derived in Supplementary Materials [Equations (S42), (S54) and (S55), respectively].

FACS analysis

Blood samples were obtained with ethical and institutional approvals (Wandsworth Research Ethics Committee, REC number 09/H0803/154). T cells were purified from blood samples from healthy volunteers after informed consent. Purified human CD4+ T cells were activated with plate-immobilized antibodies to human CD3 (Okt3) and CD46 (TRA-2-10) in the presence of 50U/ml rhIL-2 for 36 hours and the percentage of STAT3p- and STAT5p-positive cells assessed by FACS analysis. Cells were analyzed either as a bulk population or after

subsorting populations into the three IFN-γ +/- IL-10-secreting populations generated by CD3/CD46-activation. STAT3p and STAT5p values were normalized against respective non-phosphorylated STAT protein levels. Standard deviation was calculated for three independently performed experiments using a different donor each time.

48-well plates (Greiner, 677180) were coated overnight with 125 microliter/well of anti-CD3 (OKT3, BD Biosciences, 2mg/ml) and anti-CD46 (TRA-2-10, BioLegend) diluted in 1 x PBS with CaCl and MgMl (Sigma, D8862) at 4^0C to a working concentration of 2 mg/ml of each antibody. CD4+ T cells were isolated from freshly drawn blood of healthy donors using the CD4+ Magnetic Bead Kit from Miltenyi Biotec (130-045-101) as per manufacturer's protocol and plated at 500,000 cells/well in RPMI containing 10 % FCS, 2 mM Glutamine and penicillin and streptomycin. Cell were incubated for 36 hrs and then stained for actively IFN-g and/or IL-10-secreting living cells using the BD A Miltenyi Biotec human IL-10 Secretion Assay [Cell Enrichment and Detection (APC) Kit] and IFN-g Secretion Assay (FITC) in combination according to manufacturer's instructions. Cells were subsequently permeabilized (BD Cytofix/Cytoperm Kit) and then stained for non-phosphorylated STAT3 and STAT5 [anti-STAT3-PE, R+D Systems (MAB1799P); anti-STAT5a/b, LifeSpan BioSciences, Inc., (LS-C39271-100)] and for phosphorylated STAT3 and STAT5 [anti-pSTAT3 (Y705), Abcam (ab76315); anti-pSTAT5-AlexaFluor 647 (pY694), BD, 562076] in combination with appropriate secondary antibodies (anti-rabbit Violet 450 or AlexaFluor 750, all from BD Biosciences) and analyzed on the BD LSRFORTESSA machine (BD Biosciences) using the FlowJo 9.1 version (FLOWJO, LLC) for data analysis.

Results

A new integrative approach for STAT signaling

In this section, a new integrative approach is described that was used to build the systems model. Fig 1A summarizes previously published experimental results (30-45) and schematically represents the interdependent events in the cytokine/JAK-STAT signaling pathways (please see Section 1, "Integration of multiple STAT pathways" in Supplementary Materials for more details). The diagram shows which cytokines activate the known STAT proteins and illustrates the fact that the STAT proteins form homodimers as well as heterodimers only with their dimerization partners (10). In our model, STAT1 interacts with STAT2, STAT3 and STAT4 only, which is consistent with (40-42). Heterodimerization partners for STAT3 are STAT4 and STAT5. STAT4 forms a heterodimer complex with STAT3 and STAT5 whereas the only partner for STAT6 is STAT2 (43-45).

The direct result of the described experimental data integration followed by systems biology analysis is the proposition that cytokine-dependent STAT interactions lead to switching between two tightly regulated systems: the inflammatory IFN-γ only Th1 state into the regulatory Tr1 state characterized by increased IL-10 and decreased IFN-γ production levels (24).

Due to the relative complexity of Fig 1A, the scheme was divided into the two subsystems, STAT3-STAT5 and STAT3-STAT4 (Fig 1B and Fig 1C respectively), in such a way that one STAT in each pairing induces the expression of IFN-γ while the other induces the expression of IL-10. Here we only focused on the STAT pairings that produce the opposite (inflammatory and regulatory) immune responses.

In contrast to the STAT3 and STAT5 pairing (Fig 1B), where IL-2 activates both STAT3 and STAT5, in the STAT3-STAT4 system (Fig 1C), IL-2 activates only STAT3 and not STAT4. Due to this role of IL-2 in STAT3, STAT4 and STAT5 activation, we studied the effects of

variable IL-2 concentration assuming the continuous presence of the other input cytokines (IL-6, IL-21, IL-12 and IL-35) by fixing their concentrations at constant levels. As a result, the complicated scheme depicted in Fig 1A was divided into the two functionally similar but architecturally different submodules shown in Fig 1B and Fig 1C that can now be described mathematically. The mathematical description can be found in Materials and Methods and in Supplementary Materials (Section 2, "Mathematical model").

The model for coupled STAT3-STAT5 signal transduction

We started our analysis with the STAT3-STAT5 system as illustrated in Fig 1B. To build a model for the STAT3-STAT5 molecular system, we included more biological details into the description of the molecular mechanism such as cytokine-receptor interactions, STAT phosphorylation/dimerization, CD46/SP1 signaling and cytokine production. The description of the governed reactions and equations can be found in Materials and Methods and in Supplementary Materials (Section 2.1, "Model for the STAT3-STAT5 circuit").

Using optimization procedures, we obtained a set of parameters to fit our model to the experimental data for IL-2 dependent IFN-γ and IL-10 production in Th1/Tr1 switching. The data were taken from (46) and are represented in Fig 2A as circles and crosses for the normalized IFN-γ and IL-10 concentrations as a function of IL-2 respectively. The details of parameter optimization, the set of optimized parameters and parameter sensitivity analysis are described in Supplementary Materials (Section 3, "Model parameters", Fig S1 – Fig S6 and Table S2 – Table S5). Solid lines in Fig 2A illustrate the model predictions for the optimized set of parameters (set "O3" in Table S2).

Fig 2A visually demonstrates a good fit to the experimental data from (46), which is quantitatively supported by the small squared error (Table S2 in Supplementary Materials). The

figure also shows that with an increase of IL-2, the concentration of IFN-γ initially increases reaching a peak and then decreases while the concentration of IL-10 gradually increases, which leads to the switching between Th1 and Tr1 populations. At the same time, there is a population that produces both IFN-γ and IL-10, the origin of which has not yet been established (24).

Next, we hypothesized that the experimentally established IFN-γ to IL-10 switching (Fig 2A) is due to the STAT competition and caused by the STAT switching. We tested this hypothesis by comparing the model predictions with experimental data for the phosphorylated STAT monomers.

Fig 2B shows the model predictions (solid lines) for the STAT redistribution. For low IL-2 concentrations STAT5 is more highly phosphorylated than STAT3, whereas for higher IL-2 concentrations phosphorylated STAT3 prevails over STAT5. To test our model predictions experimentally, we used FACS analysis. Cells were subsorted into the three populations, namely IFN-γ only, IFN-γ/IL-10 and IL-10 only secreting cells. The levels of phosphorylated STAT3p and pSTAT5p [normalized to total STAT3 and STAT5, which was not affected by CD46 activation (not shown)] were measured in these three cell populations (Fig S7). Fig 2B shows that the model predictions are consistent with the experimental data for STAT3 and STAT5 phosphorylation levels in the corresponding cell populations. We also tested the hypothesis statistically by variation of the model parameters (see details in Supplementary Materials, Section 3.2, “Parameter sensitivity analysis”). The parameter sensitivity analysis (Fig S3) shows that the switching is still present with higher probability (more than 50%) when the parameters are perturbed within 2-fold, with modest probability (between 10% and 50%) when the parameters are perturbed within 3-6-fold and with low probability (less than 10%) when the parameters are perturbed within 7-fold and higher.

Fig 2C illustrates the model predictions for the STAT3:STAT3 and STAT5:STAT5 dimers, normalized by the total STAT3, on IL-2 concentration. The shapes of the curves for the dimers (Fig 2C) are similar to the shapes of their monomers (Fig 2B) due to the high dependence of the dimer concentrations on their monomers. Our model also predicts the bell-shaped dependence of phosphorylated STAT5 on IL-2 as well as STAT5:STAT5 homodimers on IL-2. This bell-shaped dependence suggests that STAT5 is selective to IL-2, or in other words, STAT5 has its maximum activity for a certain range of IL-2, where STAT5 phosphorylation level is high.

Investigation of possible mechanisms of JAK-STAT mediated inflammatory pathologies

We applied the developed model to investigate potential deviations in the immune system caused by changes in the tightly-regulated JAK-STAT signaling pathways. Fig 3A illustrates the influence of changes in STAT pathways on IL-10 production. The model predicts that the production of IL-10 can be increased by attenuating the removal of IL-10 by the factors of degradation (increase of our model parameters n_9 and M_{20}) as shown in Fig 3A. The changes in Fig 3A are illustrated for 15% parameter perturbation of n_9.

Our model suggests that the production of pro-inflammatory IFN-γ can be controlled by various intracellular mechanisms. For example, our model predicts (Fig 3B) that the magnitude of IFN-γ can be reduced by attenuation of the STAT5 pathway signaling (decrease of $s5_t$) (50) or by enhancement of the degradation of the produced IFN-γ (decrease of M_{18} and n_8). This may appear to be an expected result as it follows from the structure of the model shown in (Fig 1B). However, another prediction of the model is that changes in the STAT3 pathway can also reduce the level of the STAT5-activated production of IFN-γ, which is not obvious from Fig 1B. This effect could be achieved by enhancing the formation of the STAT3:STAT5 heterodimer complex (decrease of M_{14}) or alternatively by attenuation of STAT3

dephosphorylation (increase of M_9). Fig 3B shows the effects of perturbations of these model parameters for a 1.5-fold change of M_9.

As a result of the parametric alterations, the shape of IFN-γ dependence shifts along the IL-2 axis (Fig 3C). According to our model, the alterations of the parameters that cause the IFN-γ dependence shown in Fig 3C to shift to higher IL-2 concentrations represent the changes in IL-2 receptor activation. These changes include a decrease of the total amount of IL-2R (decrease of $r2_t$) or enhancement of the dephosphorylation of phosphorylated IL-2R by SHP-1 (decrease of n_1). It is notable that although the peak shifts along the IL-2 axis, the magnitude does not change during this transformation. Fig 3C shows the effects of n_1 perturbation of one order of its magnitude.

The proposed model suggests new potential strategies for the control of IFN-γ selectivity on IL-2 concentration. According to the model predictions, the IFN-γ peak shift along the IL-2 axis can be also achieved by alterations in the competing STAT3 signaling pathway (51), namely by IL-2 mediated STAT3 phosphorylation (parameter M_7) as shown in Fig 3D. This effect is a result of indirect interactions due to the redistribution of the STAT complexes as STAT3 does not directly regulate IFN-γ production. Our model predicts that due to the competition effects between STATs, STAT3 indirectly inhibits STAT5, which induces the production of IFN-γ.

The developed model also suggests that attenuation of IL-2-induced phosphorylation of STAT5 (increase of M_{10}) reduces IFN-γ magnitude and shifts the peak to the range of higher IL-2 concentrations (52-54) (Fig 3E). Our model predicts that the peak disappears when we apply the opposite changes (decrease of M_{10}). The effects of the parametric changes on the concentrations of produced IFN-γ and IL-10 are summarized in Supplementary Materials Table

S3 (the color of the arrows in Table S3 corresponds to the color of the arrows that represent changes shown in Fig 3).

The developed model also predicts how variations in the concentration of IL-6 (Fig 1B) can affect the switching (Fig 3F- Fig 3G). In our model, the concentration of IL-6 is described by parameter Q_6 as shown in Equation (6). Fig 3F illustrates that a decrease in IL-6 (Q_6 decrease) leads to stronger STAT5 to STAT3 switching, whereas an increase in IL-6 concentration (Q_6 increase) causes changes in both STAT3 and STAT5 phosphorylation levels as a function of IL-2 and thereby the lack of switching. It can be seen from Fig 3F that IL-6 activates STAT3 but at the same time inhibits STAT5 due to the STAT competition, which is consistent with observations in (55). Due to the role of IL-6 in the STAT competition (Fig 3F), IL-6 also affects the STAT-mediated production of IFN-γ and IL-10 (Fig 3G). In particular, our model predicts that due to the redistribution between STAT3 and STAT5, increased concentrations of IL-6 lead to the reduced level of pro-inflammatory IFN-γ production.

Comparative analysis of STAT3-STAT4 versus STAT3-STAT5 machinery

In this section, we further study the effects of STAT redistribution on the cytokines switching by investigating the STAT3-STAT4 circuit (Fig 1C). The cytokines that activate STAT4 include IL-12 and IL-35. In our *in silico* experiment, we studied the STAT3-STAT4 circuit for variable IL-2 concentrations and constant concentrations of IL-12, IL-35 and IL-6. A detailed description of the model for STAT3-STAT4 subsystem can be found in Supplementary Materials (Section 2.2, “Model for the STAT3-STAT4 circuit”).

In absence of any experimental data for STAT4 signaling, we assumed that the parameters in the STAT3-STAT4 subsystem are similar to the parameters in the STAT3-STAT5 subsystem (Table S4). Fig 4A-Fig 4C show the model predictions for the STAT3-STAT4 subsystem (Fig

1C). The predictions include the competition between STAT3, STAT4 monomers (Fig 4A), STAT3:STAT3 and STAT4:STAT4 homodimers (Fig 4B) as well as IFN-γ and IL-10 dependences on IL-2 concentration (Fig 4C). Despite the fact that IL-2 does not affect phosphorylation of STAT4 in the STAT3-STAT4 circuit, the switching is nonetheless present in this submodule.

It should be noted, however, that the model predictions significantly differ between these two circuits for low IL-2 concentrations. The STAT3-STAT5 circuit demonstrates the bell shaped characteristics with the low IFN-γ production for the low amounts of IL-2 (Fig 2A), whereas STAT3-STAT4 circuit reveals the significant "background" level of IFN-γ (Fig 4C). Fig 4A shows that for low IL-2 concentrations there is also a basal phosphorylation level of STAT4. Our model suggests that these "background" levels of STAT4p (Fig 4A) and subsequent IFN-γ production (Fig 4C) are due to the STAT4 activation by the maintained initial concentrations of IL-12 and IL-35 (33).

After establishing the individual properties of the STAT pathways, we next combined the two STAT3-STAT4 and STAT3-STAT5 circuits (Fig 5A). One of the major differences between the full circuit and the smaller submodules is that in the full circuit, STAT3 competes with both STAT4 and STAT5 at the same time (Fig 5B and Fig 5E) while in the smaller submodules it competes only with either at a time. The detailed description of the model for STAT3-STAT4-STAT5 subsystem is shown in Supplementary Materials (Section 2.3, "Combined STAT3-STAT4-STAT5 model"). The parameters were taken from the corresponding individual modules and are shown in Tables S1 and S2 in Supplementary Materials.

Fig 5B-Fig 5G illustrate the model predictions for the combined STAT3-STAT4-STAT5 circuit. In the range of low IL-2 concentrations, our model demonstrates two possible scenarios for IFN-γ and IL-10 production depending on which of the two phosphorylated STATs, STAT4 or STAT5, prevails. Fig 5B-Fig 5D show that the combined model predictions qualitatively coincide with the predictions for the STAT3-STAT5 subsystem (Fig 2) when the amount of phosphorylated STAT4 is significantly reduced in comparison to phosphorylated STAT5. In our model, the reduction of STAT4p is the result of an increase in the total PTP phosphatase concentration. The case shown in Fig 5E-Fig 5G, where STAT5p is strongly dephosphorylated by increased SHP-2, suggests that the response of the combined model is similar to that of STAT3-STAT4 circuit considered previously (Fig 4). For this system, we observed a significant (compared with phosphorylated STAT5) basal level of STAT4 phosphorylation (Fig 5E) as well as the "background" IFN-γ production (Fig 5G).

Thus, our model demonstrates that the IFN-γ to IL-10 switching is still present in the combined model (Fig 5D and Fig 5G). However, in the combined model, in addition to STAT3 competition with STAT4 and STAT5, there is also a competition between STAT4 and STAT5, which leads to the STAT3-STAT4- or STAT3-STAT5-like responses for the low IL-2 concentrations.

Discussion

In this paper, we developed a new integrative model to study complex STAT-STAT interactions in the JAK-STAT pathways (Fig 1). The proposed model was employed to explain the T cell phenotype plasticity effects using an example of Th1 to Tr1 switching (24). The model is consistent (Fig 2A) with the previously published experimental data for IFN-γ and IL-10 production (46). Our model suggests that the IFN-γ to IL-10 switching and the associated T cell plasticity are due to the underlying competition and redistribution of phosphorylated

STATs, which is also supported by the new experimental observations (Fig 2B and Fig S7). The analysis of our model shows that as a result of this competition, the competing STAT species can indirectly inhibit each other (Fig 2B). Moreover, the model suggests that the switching should be due to the competition between STAT species rather than competition for the source of activating cytokine. This conclusion is supported by the structure of the STAT3-STAT4 scheme (Fig 2C), where IL-2 activates only STAT3 in the pairing. Mechanistically, the competition and redistribution between STATs are implemented by the formation of STAT heterodimer complexes.

The necessity of heterodimer complex formation and their functional implications is as yet not clearly understood (33). According to our model, the role of the STAT heterodimers is to provide a "buffer", which allows the redistribution of the STAT homodimer complexes. In our model schematically shown in Fig 1A, we assumed that the STAT homodimers are more effective in mediating gene induction and therefore have a greater contribution to cytokine production compared with the heterodimers, which is consistent with (56). Therefore, we proposed that the competition between the STAT homodimers might define the type of produced cytokine and, thereby, the T cell phenotype. Our model suggests that there is a natural balance between STAT homo- and hetero- dimers. When there is no signal to switch (which corresponds to a certain concentration of input cytokines), the ratio between the homodimers is balanced. After the T cell receives the signal to switch, this balance is disrupted and then restored again, however there is now a new ratio between the competing STATs. This newly balanced ratio between the STAT homo- and hetero- dimers leads to the new type of produced cytokine and to the T cell phenotype switching. It should be noted that this is a model suggestion requiring further experimental confirmation.

External and internal factors can alter the model parameters as well as the biomolecular interactions in JAK-STAT signaling pathways. As a result, this can affect the levels of produced cytokines and the T cell phenotype. We investigated how these alterations (possibly caused by genetic mutations) can lead to various pathological states without changing the structure of the model (Fig 3). Immune-related pathologies caused by *Leishmania major* or Epstein-virus are associated with an inappropriate balance between pro-inflammatory and anti-inflammatory cytokines (57, 58). Our model predictions demonstrate possible scenarios of alterations in JAK STAT pathways that affect IL-10 (Fig 3A) and IFN-γ production (Fig 3B and Fig 3C) as well as the selective regulation of IFN-γ by IL-2 (Fig 3D and Fig 3E). The model predicts that inappropriate regulation of the IL-2 receptor system leads to the dysfunctions of the IFN-γ to IL-10 switching (Fig 3C), which in turn can mediate autoimmune states such as IBD (24, 59). A number of pharmacological and clinical studies have demonstrated aberrant STATs activation in human tumor diseases. It was reported that the inhibition of STAT3 is a promising strategy for anti-cancer treatment (22, 23, 60). However, there is still a limited understanding of the underlying mechanisms of this inhibition. Our model proposes alternative, interdependent strategies for the regulation of IFN-γ and IL-10 production by employing their competing STAT pathways (Fig 3A-Fig 3E). The model predictions suggest that the inhibitor selectivity to specific STAT proteins might enhance the anti-cancer effect.

The molecular mechanisms underlying STAT signaling have been a subject of extensive systems biology research in recent years. A mathematical model of JAK-STAT signaling pathway leading to the activation of STAT1 in liver cells was proposed in (26). Another attempt to model STAT1 activation was made in (27) studying JAK-STAT signaling in pancreatic stellate cells (PSC). In (28), a mathematical model for the JAK2-STAT5 pathway was proposed. Importantly, in the studies (26-28), only one JAK-STAT pathway was

investigated at a time. This fact limits the application of these models to phenotype development and plasticity in response to environmental changes in T-cells, where more than one JAK-STAT pathways are involved (24, 61). The first attempt to introduce the crosstalk between STAT pathways into a systems model, was published in (62). Using an example of STAT1 and STAT3 pathways, the importance of the crosstalk and STAT1:STAT3 heterodimer formation was highlighted in that study. However, the model (62) only considered the dynamics of the STAT system and did not include the production of cytokines, which also rather limits the application of the model to phenotype formation and plasticity involved in a variety of immune diseases.

The fact that our model considers multiple JAK-STAT pathways at a time also provides new insights into the interpretation of some of the conflicting experimental results (50, 53, 63-65) (30, 31, 39, 66). For example, in (50, 53, 63), it was shown that the activated STAT5 leads to the production of IFN-γ, while in (64), it was demonstrated that IL-10 production is also enhanced through STAT5 activation. At the same time, the fact that STAT4 activates IFN-γ production (30, 31, 39) contradicts with the data in (66), where it was shown that STAT4 also induces the production of IL-10. The proposed model offers potential explanation of this duality in experimental data by introducing the selectivity in JAK-STAT pathways depending on IL-2 concentration (Fig 2).

In our work, we focused on one example of pro-inflammatory IFN-γ and regulatory IL-10 production in the Th1/Tr1 phenotype switching via STAT proteins. However, it should be noted that the considered STATs shown in Fig 1A, can also induce the production of cytokines other than IFN-γ and IL-10. Therefore, the proposed model can be potentially applied to describe the plasticity effects and the switching not only between Th1 and Tr1, but also other T cell phenotypes such as Th1/Th2 (67), Treg/Th17 and Th17/Th2 (68) phenotype switching.

Acknowledgements

Author contributions

IIS developed and implemented the project under the supervision of NVK, MZQC, CK, VNB, GIW and YU. CK generated and provided the experimental data pertaining to the status of STAT activation and phosphorylation in T cells. All authors contributed to the analysis of the model. CK, YU, DVS and GIW provided biological interpretations of the results. All authors contributed to the writing of the final manuscript. All authors have read and approved the final version of the manuscript.

Funding

This work was carried out under Severnside Alliance for Translational Research (SARTRE) grant (GIW) and NSFC grant 61374053 (MZQC). This work was co-funded by the subsidy allocated to the Kazan Federal University for state assignment in the sphere of scientific activities and performed according to the 'Russian Government Program of Competitive Growth' of the Kazan Federal University.

Conflict of interest

The authors declare that they have no conflict of interest.

References

1. Lin J, Buettner R, Yuan YC, Yip R, Horne D, Jove R, et al. Molecular dynamics simulations of the conformational changes in signal transducers and activators of transcription, Stat1 and Stat3. Journal of molecular graphics & modelling. 2009 Nov;28(4):347-56. PubMed PMID: 19781967.
2. Calo V, Migliavacca M, Bazan V, Macaluso M, Buscemi M, Gebbia N, et al. STAT proteins: from normal control of cellular events to tumorigenesis. Journal of cellular physiology. 2003 Nov;197(2):157-68. PubMed PMID: 14502555.
3. Sadzak I, Schiff M, Gattermeier I, Glinitzer R, Sauer I, Saalmuller A, et al. Recruitment of Stat1 to chromatin is required for interferon-induced serine phosphorylation of Stat1 transactivation domain.

Proc Natl Acad Sci U S A. 2008 Jul 1;105(26):8944-9. PubMed PMID: 18574148. Pubmed Central PMCID: 2435588. Epub 2008/06/25. eng.
4. Sakaguchi M, Oka M, Iwasaki T, Fukami Y, Nishigori C. Role and regulation of STAT3 phosphorylation at Ser727 in melanocytes and melanoma cells. J Invest Dermatol. 2012 Jul;132(7):1877-85. PubMed PMID: 22418867. Epub 2012/03/16. eng.
5. Niemand C, Nimmesgern A, Haan S, Fischer P, Schaper F, Rossaint R, et al. Activation of STAT3 by IL-6 and IL-10 in primary human macrophages is differentially modulated by suppressor of cytokine signaling 3. J Immunol. 2003 Mar 15;170(6):3263-72. PubMed PMID: 12626585. Epub 2003/03/11. eng.
6. Schuringa JJ, Wierenga AT, Kruijer W, Vellenga E. Constitutive Stat3, Tyr705, and Ser727 phosphorylation in acute myeloid leukemia cells caused by the autocrine secretion of interleukin-6. Blood. 2000 Jun 15;95(12):3765-70. PubMed PMID: 10845908. Epub 2000/06/14. eng.
7. Liu YP, Tan YN, Wang ZL, Zeng L, Lu ZX, Li LL, et al. Phosphorylation and nuclear translocation of STAT3 regulated by the Epstein-Barr virus latent membrane protein 1 in nasopharyngeal carcinoma. Int J Mol Med. 2008 Feb;21(2):153-62. PubMed PMID: 18204781. Epub 2008/01/22. eng.
8. Aggarwal BB, Kunnumakkara AB, Harikumar KB, Gupta SR, Tharakan ST, Koca C, et al. Signal transducer and activator of transcription-3, inflammation, and cancer: how intimate is the relationship? Ann N Y Acad Sci. 2009 Aug;1171:59-76. PubMed PMID: 19723038. Pubmed Central PMCID: 3141289. Epub 2009/09/03. eng.
9. Darnell JE, Jr. STATs and gene regulation. Science. 1997 Sep 12;277(5332):1630-5. PubMed PMID: 9287210. Epub 1997/09/12. eng.
10. Au-Yeung N, Mandhana R, Horvath CM. Transcriptional regulation by STAT1 and STAT2 in the interferon JAK-STAT pathway. Jak-Stat. 2013 Jul 1;2(3):e23931. PubMed PMID: 24069549. Pubmed Central PMCID: 3772101.
11. Barry SP, Townsend PA, Latchman DS, Stephanou A. Role of the JAK-STAT pathway in myocardial injury. Trends in molecular medicine. 2007 Feb;13(2):82-9. PubMed PMID: 17194625.
12. Mitchell TJ, John S. Signal transducer and activator of transcription (STAT) signalling and T-cell lymphomas. Immunology. 2005 Mar;114(3):301-12. PubMed PMID: 15720432. Pubmed Central PMCID: 1782085.
13. Husby J, Todd AK, Haider SM, Zinzalla G, Thurston DE, Neidle S. Molecular dynamics studies of the STAT3 homodimer:DNA complex: relationships between STAT3 mutations and protein-DNA recognition. Journal of chemical information and modeling. 2012 May 25;52(5):1179-92. PubMed PMID: 22500887.
14. Kershaw NJ, Murphy JM, Liau NP, Varghese LN, Laktyushin A, Whitlock EL, et al. SOCS3 binds specific receptor-JAK complexes to control cytokine signaling by direct kinase inhibition. Nature structural & molecular biology. 2013 Apr;20(4):469-76. PubMed PMID: 23454976. Pubmed Central PMCID: 3618588.
15. Lubberts E, van den Berg WB. Cytokines in the pathogenesis of rheumatoid arthritis and collagen-induced arthritis. Advances in experimental medicine and biology. 2003;520:194-202. PubMed PMID: 12613579.
16. Chomarat P, Vannier E, Dechanet J, Rissoan MC, Banchereau J, Dinarello CA, et al. Balance of IL-1 receptor antagonist/IL-1 beta in rheumatoid synovium and its regulation by IL-4 and IL-10. Journal of immunology. 1995 Feb 1;154(3):1432-9. PubMed PMID: 7822808.
17. Sule S, Rosen A, Petri M, Akhter E, Andrade F. Abnormal production of pro- and anti-inflammatory cytokines by lupus monocytes in response to apoptotic cells. PloS one. 2011;6(3):e17495. PubMed PMID: 21423726. Pubmed Central PMCID: 3056659.
18. Sivalingam SP, Thumboo J, Vasoo S, Thio ST, Tse C, Fong KY. In vivo pro- and anti-inflammatory cytokines in normal and patients with rheumatoid arthritis. Annals of the Academy of Medicine, Singapore. 2007 Feb;36(2):96-9. PubMed PMID: 17364074.
19. Dean GS, Tyrrell-Price J, Crawley E, Isenberg DA. Cytokines and systemic lupus erythematosus. Annals of the rheumatic diseases. 2000 Apr;59(4):243-51. PubMed PMID: 10733469. Pubmed Central PMCID: 1753117.
20. Russell MA, Cooper AC, Dhayal S, Morgan NG. Differential effects of interleukin-13 and interleukin-6 on Jak/STAT signaling and cell viability in pancreatic beta-cells. Islets. 2013 Mar-Apr;5(2):95-105. PubMed PMID: 23510983.
21. Kaminski A, Welters HJ, Kaminski ER, Morgan NG. Human and rodent pancreatic beta-cells express IL-4 receptors and IL-4 protects against beta-cell apoptosis by activation of the PI3K and JAK/STAT pathways. Bioscience reports. 2010 Jun;30(3):169-75. PubMed PMID: 19531027.
22. Nelson EA, Sharma SV, Settleman J, Frank DA. A chemical biology approach to developing STAT inhibitors: molecular strategies for accelerating clinical translation. Oncotarget. 2011 Jun;2(6):518-24. PubMed PMID: 21680956. Pubmed Central PMCID: 3248200.

23. Hayakawa F, Sugimoto K, Harada Y, Hashimoto N, Ohi N, Kurahashi S, et al. A novel STAT inhibitor, OPB-31121, has a significant antitumor effect on leukemia with STAT-addictive oncokinases. Blood cancer journal. 2013;3:e166. PubMed PMID: 24292418. Pubmed Central PMCID: 3880446.
24. Cope A, Le Friec G, Cardone J, Kemper C. The Th1 life cycle: molecular control of IFN-gamma to IL-10 switching. Trends in immunology. 2011 Jun;32(6):278-86. PubMed PMID: 21531623.
25. Magombedze G, Reddy PB, Eda S, Ganusov VV. Cellular and population plasticity of helper CD4(+) T cell responses. Frontiers in physiology. 2013;4:206. PubMed PMID: 23966946. Pubmed Central PMCID: 3744810.
26. Yamada S, Shiono S, Joo A, Yoshimura A. Control mechanism of JAK/STAT signal transduction pathway. FEBS letters. 2003 Jan 16;534(1-3):190-6. PubMed PMID: 12527385.
27. Rateitschak K, Karger A, Fitzner B, Lange F, Wolkenhauer O, Jaster R. Mathematical modelling of interferon-gamma signalling in pancreatic stellate cells reflects and predicts the dynamics of STAT1 pathway activity. Cellular signalling. 2010 Jan;22(1):97-105. PubMed PMID: 19781632.
28. Swameye I, Muller TG, Timmer J, Sandra O, Klingmuller U. Identification of nucleocytoplasmic cycling as a remote sensor in cellular signaling by databased modeling. Proceedings of the National Academy of Sciences of the United States of America. 2003 Feb 4;100(3):1028-33. PubMed PMID: 12552139. Pubmed Central PMCID: 298720.
29. Sadreev, II, Chen MZ, Welsh GI, Umezawa Y, Kotov NV, Valeyev NV. A systems model of phosphorylation for inflammatory signaling events. PloS one. 2014;9(10):e110913. PubMed PMID: 25333362. Pubmed Central PMCID: 4205014.
30. Guo L, Junttila IS, Paul WE. Cytokine-induced cytokine production by conventional and innate lymphoid cells. Trends in immunology. 2012 Dec;33(12):598-606. PubMed PMID: 22959641.
31. Strengell M, Matikainen S, Siren J, Lehtonen A, Foster D, Julkunen I, et al. IL-21 in synergy with IL-15 or IL-18 enhances IFN-gamma production in human NK and T cells. Journal of immunology. 2003 Jun 1;170(11):5464-9. PubMed PMID: 12759422.
32. Kasahara T, Hooks JJ, Dougherty SF, Oppenheim JJ. Interleukin 2-mediated immune interferon (IFN-gamma) production by human T cells and T cell subsets. Journal of immunology. 1983 Apr;130(4):1784-9. PubMed PMID: 6403613.
33. Delgoffe GM, Vignali DA. STAT heterodimers in immunity: A mixed message or a unique signal? Jak-Stat. 2013 Jan 1;2(1):e23060. PubMed PMID: 24058793. Pubmed Central PMCID: 3670269.
34. Scheeren FA, Diehl SA, Smit LA, Beaumont T, Naspetti M, Bende RJ, et al. IL-21 is expressed in Hodgkin lymphoma and activates STAT5: evidence that activated STAT5 is required for Hodgkin lymphomagenesis. Blood. 2008 May 1;111(9):4706-15. PubMed PMID: 18296629. Pubmed Central PMCID: 2343600.
35. Gilmour KC, Pine R, Reich NC. Interleukin 2 activates STAT5 transcription factor (mammary gland factor) and specific gene expression in T lymphocytes. Proceedings of the National Academy of Sciences of the United States of America. 1995 Nov 7;92(23):10772-6. PubMed PMID: 7479881. Pubmed Central PMCID: 40694.
36. Sanz E, Hofer MJ, Unzeta M, Campbell IL. Minimal role for STAT1 in interleukin-6 signaling and actions in the murine brain. Glia. 2008 Jan 15;56(2):190-9. PubMed PMID: 18023015.
37. Hibbert L, Pflanz S, De Waal Malefyt R, Kastelein RA. IL-27 and IFN-alpha signal via Stat1 and Stat3 and induce T-Bet and IL-12Rbeta2 in naive T cells. Journal of interferon & cytokine research : the official journal of the International Society for Interferon and Cytokine Research. 2003 Sep;23(9):513-22. PubMed PMID: 14565860.
38. Fung MM, Rohwer F, McGuire KL. IL-2 activation of a PI3K-dependent STAT3 serine phosphorylation pathway in primary human T cells. Cellular signalling. 2003 Jun;15(6):625-36. PubMed PMID: 12681450.
39. Wurster AL, Tanaka T, Grusby MJ. The biology of Stat4 and Stat6. Oncogene. 2000 May 15;19(21):2577-84. PubMed PMID: 10851056.
40. Li X, Leung S, Qureshi S, Darnell JE, Jr., Stark GR. Formation of STAT1-STAT2 heterodimers and their role in the activation of IRF-1 gene transcription by interferon-alpha. The Journal of biological chemistry. 1996 Mar 8;271(10):5790-4. PubMed PMID: 8621447.
41. Wang WB, Levy DE, Lee CK. STAT3 negatively regulates type I IFN-mediated antiviral response. Journal of immunology. 2011 Sep 1;187(5):2578-85. PubMed PMID: 21810606.
42. Collison LW, Delgoffe GM, Guy CS, Vignali KM, Chaturvedi V, Fairweather D, et al. The composition and signaling of the IL-35 receptor are unconventional. Nature immunology. 2012 Mar;13(3):290-9. PubMed PMID: 22306691. Pubmed Central PMCID: 3529151.
43. Higashi T, Tsukada J, Yoshida Y, Mizobe T, Mouri F, Minami Y, et al. Constitutive tyrosine and serine phosphorylation of STAT4 in T-cells transformed with HTLV-I. Genes to cells : devoted to molecular & cellular mechanisms. 2005 Dec;10(12):1153-62. PubMed PMID: 16324152.

44. Tanabe Y, Nishibori T, Su L, Arduini RM, Baker DP, David M. Cutting edge: role of STAT1, STAT3, and STAT5 in IFN-alpha beta responses in T lymphocytes. Journal of immunology. 2005 Jan 15;174(2):609-13. PubMed PMID: 15634877.
45. Gupta S, Jiang M, Pernis AB. IFN-alpha activates Stat6 and leads to the formation of Stat2:Stat6 complexes in B cells. Journal of immunology. 1999 Oct 1;163(7):3834-41. PubMed PMID: 10490982.
46. Cardone J, Le Friec G, Vantourout P, Roberts A, Fuchs A, Jackson I, et al. Complement regulator CD46 temporally regulates cytokine production by conventional and unconventional T cells. Nature immunology. 2010 Sep;11(9):862-71. PubMed PMID: 20694009. Pubmed Central PMCID: 4011020.
47. Valeyev NV, Hundhausen C, Umezawa Y, Kotov NV, Williams G, Clop A, et al. A systems model for immune cell interactions unravels the mechanism of inflammation in human skin. PLoS computational biology. 2010;6(12):e1001024. PubMed PMID: 21152006. Pubmed Central PMCID: 2996319.
48. Lucas M, Zhang X, Prasanna V, Mosser DM. ERK activation following macrophage FcgammaR ligation leads to chromatin modifications at the IL-10 locus. Journal of immunology. 2005 Jul 1;175(1):469-77. PubMed PMID: 15972681.
49. Sarkar S, Han J, Sinsimer KS, Liao B, Foster RL, Brewer G, et al. RNA-binding protein AUF1 regulates lipopolysaccharide-induced IL10 expression by activating IkappaB kinase complex in monocytes. Molecular and cellular biology. 2011 Feb;31(4):602-15. PubMed PMID: 21135123. Pubmed Central PMCID: 3028643.
50. Shi M, Lin TH, Appell KC, Berg LJ. Janus-kinase-3-dependent signals induce chromatin remodeling at the Ifng locus during T helper 1 cell differentiation. Immunity. 2008 Jun;28(6):763-73. PubMed PMID: 18549798. Pubmed Central PMCID: 2587400.
51. Kimura D, Miyakoda M, Honma K, Shibata Y, Yuda M, Chinzei Y, et al. Production of IFN-gamma by CD4(+) T cells in response to malaria antigens is IL-2 dependent. International immunology. 2010 Dec;22(12):941-52. PubMed PMID: 21059770.
52. Bream JH, Hodge DL, Gonsky R, Spolski R, Leonard WJ, Krebs S, et al. A distal region in the interferon-gamma gene is a site of epigenetic remodeling and transcriptional regulation by interleukin-2. The Journal of biological chemistry. 2004 Sep 24;279(39):41249-57. PubMed PMID: 15271977.
53. Herr F, Lemoine R, Gouilleux F, Meley D, Kazma I, Heraud A, et al. IL-2 phosphorylates STAT5 to drive IFN-gamma production and activation of human dendritic cells. Journal of immunology. 2014 Jun 15;192(12):5660-70. PubMed PMID: 24829413.
54. Chen J, Yu WM, Bunting KD, Qu CK. A negative role of SHP-2 tyrosine phosphatase in growth factor-dependent hematopoietic cell survival. Oncogene. 2004 Apr 29;23(20):3659-69. PubMed PMID: 15116097.
55. Denson LA, Held MA, Menon RK, Frank SJ, Parlow AF, Arnold DL. Interleukin-6 inhibits hepatic growth hormone signaling via upregulation of Cis and Socs-3. American journal of physiology Gastrointestinal and liver physiology. 2003 Apr;284(4):G646-54. PubMed PMID: 12519742.
56. Ho HH, Ivashkiv LB. Role of STAT3 in type I interferon responses. Negative regulation of STAT1-dependent inflammatory gene activation. The Journal of biological chemistry. 2006 May 19;281(20):14111-8. PubMed PMID: 16571725.
57. Anderson CF, Oukka M, Kuchroo VJ, Sacks D. CD4(+)CD25(-)Foxp3(-) Th1 cells are the source of IL-10-mediated immune suppression in chronic cutaneous leishmaniasis. The Journal of experimental medicine. 2007 Feb 19;204(2):285-97. PubMed PMID: 17283207. Pubmed Central PMCID: 2118728.
58. Moore KW, Vieira P, Fiorentino DF, Trounstine ML, Khan TA, Mosmann TR. Homology of cytokine synthesis inhibitory factor (IL-10) to the Epstein-Barr virus gene BCRFI. Science. 1990 Jun 8;248(4960):1230-4. PubMed PMID: 2161559.
59. Malek TR, Castro I. Interleukin-2 receptor signaling: at the interface between tolerance and immunity. Immunity. 2010 Aug 27;33(2):153-65. PubMed PMID: 20732639. Pubmed Central PMCID: 2946796.
60. Furqan M, Akinleye A, Mukhi N, Mittal V, Chen Y, Liu D. STAT inhibitors for cancer therapy. Journal of hematology & oncology. 2013;6:90. PubMed PMID: 24308725. Pubmed Central PMCID: 4029528.
61. Yoshimura A, Suzuki M, Sakaguchi R, Hanada T, Yasukawa H. SOCS, Inflammation, and Autoimmunity. Frontiers in immunology. 2012;3:20. PubMed PMID: 22566904. Pubmed Central PMCID: 3342034.
62. Qi YF, Huang YX, Wang HY, Zhang Y, Bao YL, Sun LG, et al. Elucidating the crosstalk mechanism between IFN-gamma and IL-6 via mathematical modelling. BMC bioinformatics. 2013 Feb 06;14:41. PubMed PMID: 23384097. Pubmed Central PMCID: 3599299.

63. Gonsky R, Deem RL, Bream J, Young HA, Targan SR. Enhancer role of STAT5 in CD2 activation of IFN-gamma gene expression. Journal of immunology. 2004 Nov 15;173(10):6241-7. PubMed PMID: 15528362.
64. Tsuji-Takayama K, Suzuki M, Yamamoto M, Harashima A, Okochi A, Otani T, et al. The production of IL-10 by human regulatory T cells is enhanced by IL-2 through a STAT5-responsive intronic enhancer in the IL-10 locus. Journal of immunology. 2008 Sep 15;181(6):3897-905. PubMed PMID: 18768844.
65. Forsberg G, Hernell O, Melgar S, Israelsson A, Hammarstrom S, Hammarstrom ML. Paradoxical coexpression of proinflammatory and down-regulatory cytokines in intestinal T cells in childhood celiac disease. Gastroenterology. 2002 Sep;123(3):667-78. PubMed PMID: 12198691.
66. Saraiva M, Christensen JR, Veldhoen M, Murphy TL, Murphy KM, O'Garra A. Interleukin-10 production by Th1 cells requires interleukin-12-induced STAT4 transcription factor and ERK MAP kinase activation by high antigen dose. Immunity. 2009 Aug 21;31(2):209-19. PubMed PMID: 19646904. Pubmed Central PMCID: 2791889.
67. Clerici M, Shearer GM. A TH1-->TH2 switch is a critical step in the etiology of HIV infection. Immunology today. 1993 Mar;14(3):107-11. PubMed PMID: 8096699.
68. Lane N, Robins RA, Corne J, Fairclough L. Regulation in chronic obstructive pulmonary disease: the role of regulatory T-cells and Th17 cells. Clinical science. 2010 Jul;119(2):75-86. PubMed PMID: 20402669.

Figure legends

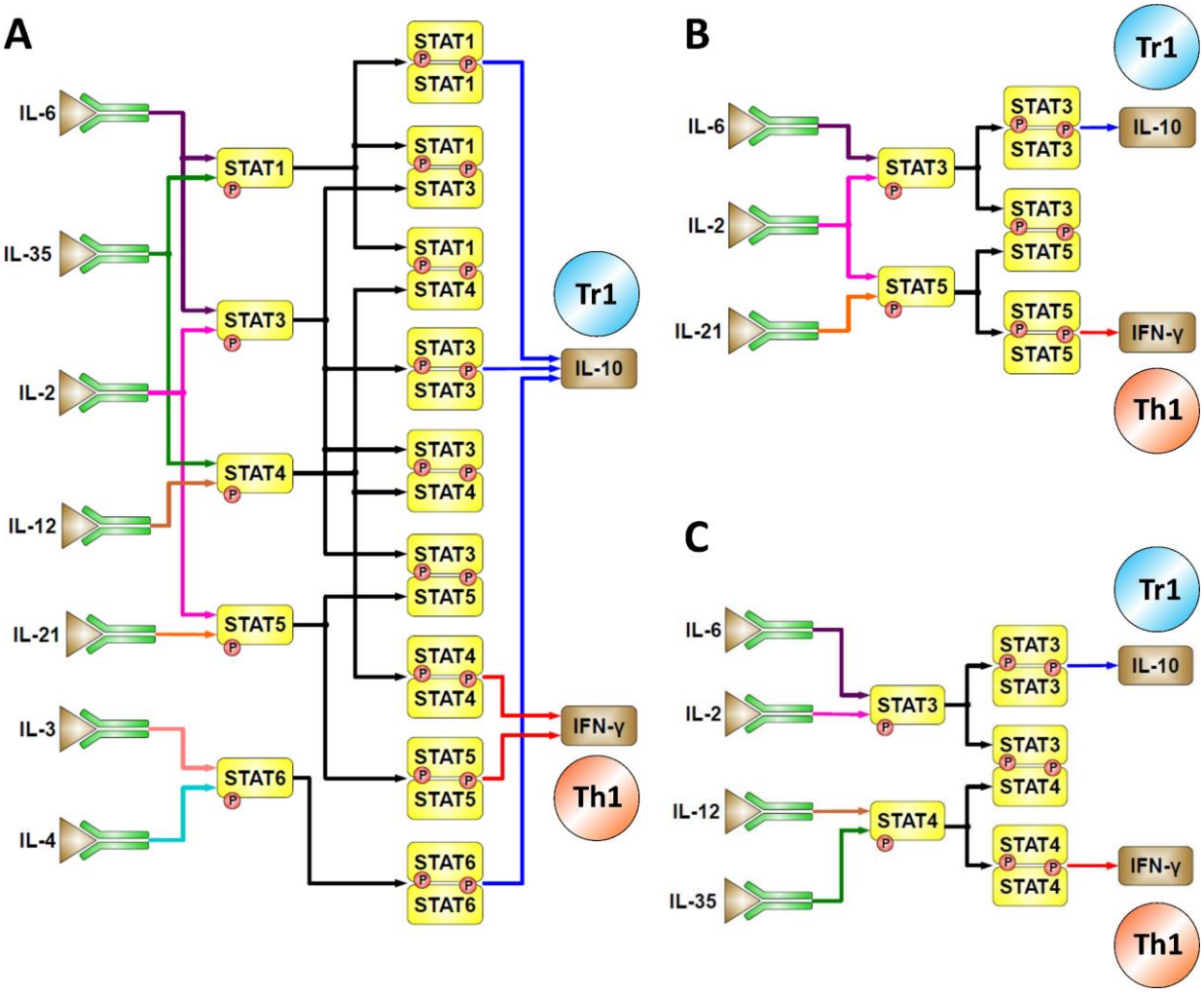

Fig 1. The map of interleukins involved in induction of IFN-γ and IL-10 production via the STAT-activating mechanisms. A. The map of interactions between the cytokines and the STATs based on

experimental studies (30-45). According to the map, STAT proteins are activated in response to extracellular cytokines. STATs can form dimer complexes only with certain dimerization partners. STAT dimers induce IFN-γ and IL-10 gene expression. B. STAT3-STAT5 subsystem extracted from the full map of interactions shown in (A). This subsystem activates IFN-γ and IL-10 production in response to IL-2, IL-6 and IL-21. In this model, IL-2 activates both STAT3 and STAT5 while the concentration of other cytokines is maintained constant. C. STAT3-STAT4 subsystem extracted from the full map (A). This subsystem induces the expression of IFN-γ and IL-10 in response to IL-2, IL-6, IL-12 and IL-35. In this case IL-2 activates STAT3 only.

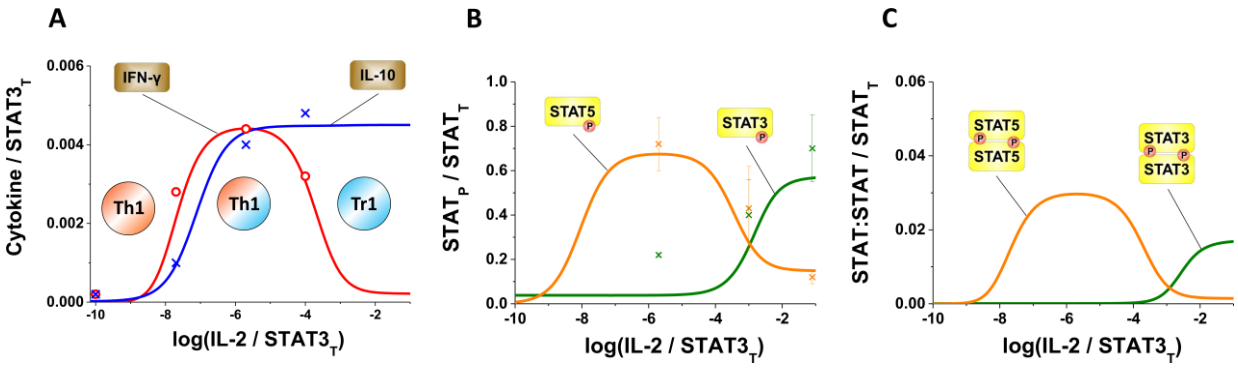

Fig 2. The IL-2-dependent IFN-γ to IL-10 switching is due to the underlying STAT competition. A. Model predictions (solid lines) compared with the experimental data for IFN-γ and IL-10 production as a function of IL-2 concentration (red circles and blue crosses respectively). Normalized experimental data from (46) show that the concentration of produced IFN-γ (circles) and IL-10 (crosses) depends on IL-2 concentration. With an increase of IL-2, the production of IFN-γ initially increases compared with the production of IL-10 for the same IL-2 concentration. Further increase of IL-2 leads to the decrease of IFN-γ and increase of IL-10 concentration. The low IL-10 and high IFN-γ correspond to the Th1 cell state, the medium IFN-γ and IL-10 concentrations correspond to the IL-10-producing Th1 cells and high IL-10 and low IFN-γ correspond to the Tr1 cell state, which is in line with the experimentally observed fact that the switching occurs for high amounts of IL-2 and that the activation of IFN-γ always precedes IL-10 (24). B. The model predicts that the IFN-γ to IL-10 switching shown in A is due to the STAT5p and STAT3p redistribution. This prediction is consistent with the experimental data (shown as x) also illustrated in Fig S7. The STAT dependencies demonstrate selective (bell-shaped) concentration-dependent STAT5 activation profile and sigmoid (dose-response) STAT3 activation profile as a function of IL-2 concentration. C. STAT5:STAT5 homodimers also show selectivity to IL-2 due to the high dependence on STAT5p.

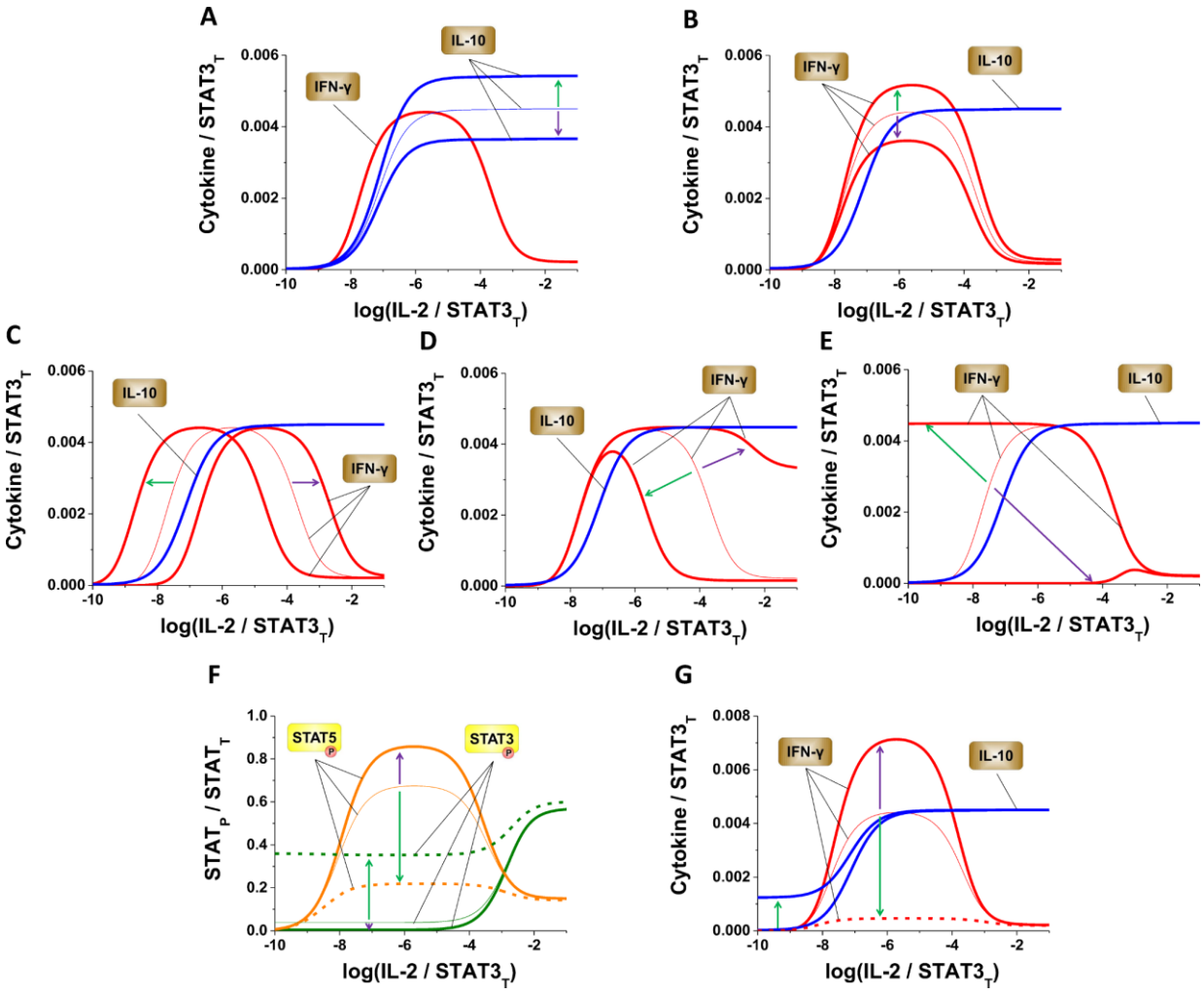

Fig 3. The effects of changes in intracellular regulation on the developed model predictions. The aberrations in both activating or competing JAK-STAT pathways regulate the amounts of produced IL-10 (A) and IFN-γ (B-E). The profile of IFN-γ production can be shifted along IL-2 axis by changes in IL-2R signaling (C). The aberrations in STAT3 and STAT5 phosphorylation may lead to IFN-γ profile shift along IL-2 axis with the reduction of its magnitude at the same time (D, E). The model predictions show that increased IL-6 leads to the lack of STAT redistribution (dotted lines in F) while reduced amount of IL-6 may lead to stronger STAT redistribution (solid lines in F). The lack of STAT redistribution observed for increased IL-6 leads to significantly lower level of IFN-γ production (G). Thus, our model predicts that the level of IFN-γ production can be reduced by the IL-6-dependent changes in the competing STAT3 pathway. Thin lines represent the model predictions for the optimized set of parameters, while solid and dotted lines show the model predictions for the perturbed parameters shown in Table S3 in Supplementary Materials.

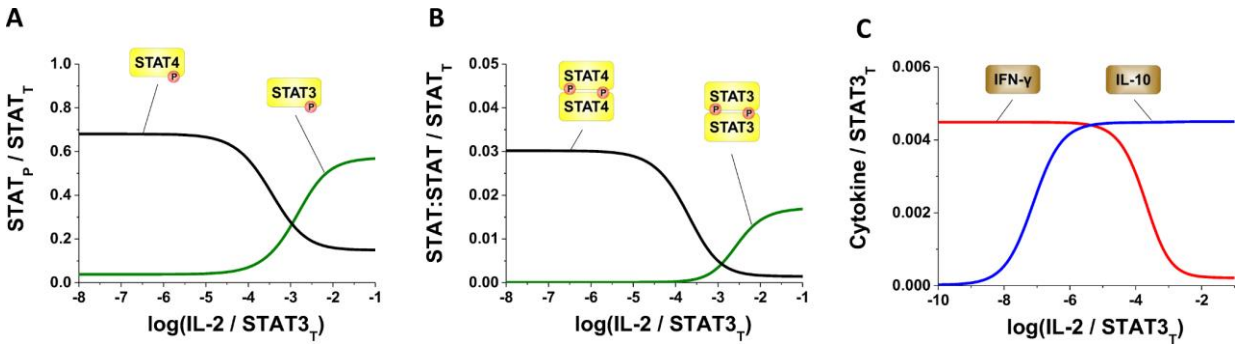

Fig 4. Model predictions for the STAT3-STAT4 circuit. Redistribution between STAT3 and STAT4 monomers (A) as well as STAT3:STAT3 and STAT5:STAT5 homodimers (B) leads to the IFN-γ to IL-10 switching for higher IL-2 concentrations shown in (C). Our model predicts that there is a significant basal level of STAT4p and thereby STAT4:STAT4 homodimer for low IL-2. This is due to the fact that in our model IL-12 and IL-35 are maintained constant while varied IL-2 activates only STAT3 and not STAT4 in this pairing. The basal STAT4:STAT4 homodimer level leads to the background level of IFN-γ production and the lack of initial co-expression between produced IFN-γ and IL-10 (C).

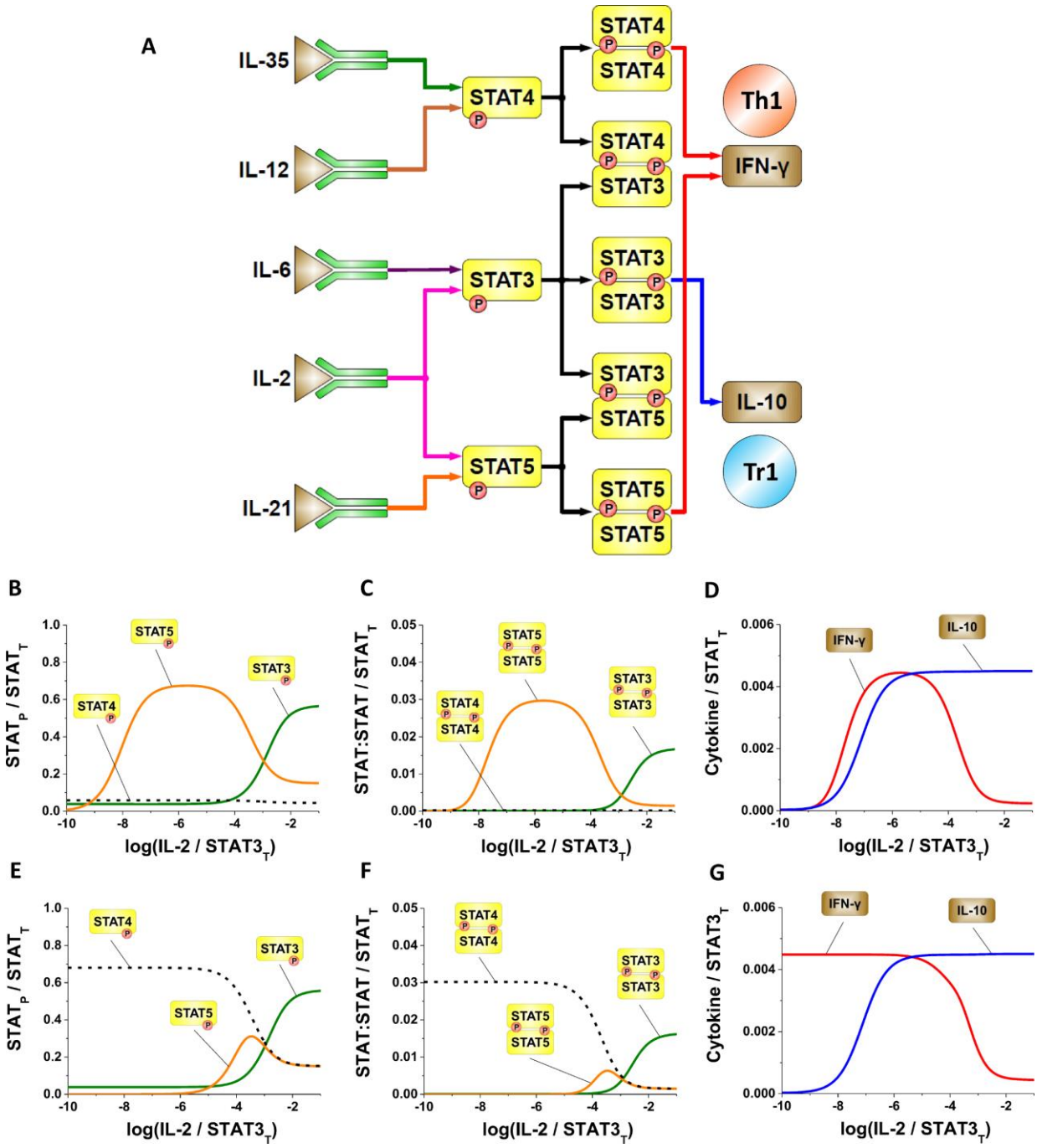

Fig 5. The model predictions for the combined STAT3-STAT4-STAT5 circuit. A. Schematic diagram for the combined STAT3-STAT4-STAT5 model. B-D. The dose-response profiles show that for significantly dephosphorylated STAT4, the STAT3-STAT5 like responses prevail and the selective production of IFN-γ arises. E-G. The model predictions for dephosphorylated STAT5 reveal STAT3-STAT4 like responses with no selectivity for IFN-γ production observed.